

Fatigue Crack Growth Rate Behavior of Tank Car Steel TC-128B

Peter C. McKeighan
James H. Feiger
Southwest Research Institute
6220 Culebra Rd.
San Antonio, TX 78238-5166
210.522.3617 (PCM) 210.522.6881 (JHF)
pmckeighan@swri.org jfeiger@swri.org

William T. Riddell
Volpe National Transportation Systems Center, DTS-76
55 Broadway
Cambridge, MA 02142-1093
617.494.2680
riddell@volpe.dot.gov

Key Words: Fatigue Crack Growth Rate, Railroad Tank Car, Structural Integrity,
TC-128B, Damage Tolerance

INTRODUCTION

As part of an effort to apply damage tolerance concepts to railroad tank cars, the fatigue crack growth (FCG) behavior of two lots of TC-128B (similar to A612 Grade B steel) steel was investigated. Advanced test control strategies were used to optimize testing, resulting in twenty-one FCG datasets using thirteen specimens. In addition to the material lot difference, variables assessed include load ratio ($R = 0.1, 0.6$ and -1.0), orientation (L-T and L-S) and, indirectly, crack growth test technique (K-decreasing, -increasing, constant- K_{\max} with increasing- K_{\min}). The two material lots yielded essentially identical FCG properties for both low and high R-ratio. The influence of R-ratio was slight, on the order of a 50 percent increase in growth rate at the higher 0.6 R-ratio when compared to low R-ratio conditions. The in-plane orientation (L-T) exhibits a growth rate approximately two times (2x) faster than the through-thickness orientation (L-S). Furthermore, constant K_{\max} test results suggest that the fatigue crack growth threshold is approximately 2-3 ksi $\sqrt{\text{in}}$ and 3-4 ksi $\sqrt{\text{in}}$ for the L-T and L-S orientation, respectively. Finally, the data generated for TC-128B in the two orientations tested (a) agrees well with A612-Gr. B data extracted from the literature and (b) exhibits slightly slower growth rates than a generalized FCG response derived for common structural and low alloy steels.

BACKGROUND

Under normal service conditions, a railroad tank car is subjected to cyclic loads that can cause structural damage to the car. Fatigue cracking and structural failures in railroad tank cars have been documented since the mid-1980s⁽¹⁾. These cracks were detected as part of an inspection program implemented by the tank car industry working in concert with the U.S. and Canadian regulatory bodies. Implementing performance-based inspection intervals could optimize safety and operating costs. Performance-based inspection intervals are based on the time that it would take the largest crack that might be missed in an inspection to grow to failure. This design approach utilizing inspection intervals is known as damage tolerance^(2,3). A damage tolerance analysis (DTA) approach is desirable because it ensures that fatigue cracking does not lead to catastrophic failure while insuring optimum maintenance efficiency by defining the periodic inspection rate. However, an accurate damage tolerant design requires extensive knowledge of the service loading conditions, material(s), local stresses and geometric influences. One of the key parameters required in this type of design is the fatigue crack growth rate behavior so that the speed of crack growth can be predicted under service loading conditions.

Paris was the first to suggest a fracture mechanics approach to predicting fatigue crack growth rates⁽⁴⁾. Paris noted a linear relationship between fatigue crack growth rate (da/dN) when plotted against cyclic stress intensity factor (ΔK) on a log-log plot. In principle, this observation allows fatigue crack growth rates observed during laboratory tests to be used in design, since nearly all models for fatigue crack growth have utilized ΔK as the primary predictor of crack growth rates. In practice, however, predicting fatigue crack growth rate requires more than simply the ΔK range since the underlying material behavior is fairly complex. For example, stress ratio (R , also called R -ratio and defined as the ratio of minimum to maximum load) and fatigue crack growth threshold (ΔK_{th}) can have considerable effect on growth rates⁽⁵⁾. The fatigue crack growth threshold is the ΔK that defines when cracks propagate; at ΔK levels below ΔK_{th} , the crack growth is effectively arrested.

Tank car steel TC-128B is used in the manufacture of tank car shells. A fatigue failure in a shell could directly result in a loss of lading; so the FCG behavior of TC-128B is of concern. The purpose of this paper is to present results from a series of tests designed to characterize fatigue crack growth behavior in TC-128B, as produced by two different manufacturers. Specifically, the effects of stress ratio, and orientation are investigated under a wide range of ΔK . These data will provide the basis for future work toward developing models for propagation of fatigue cracks under the complex stress, geometry, and environmental conditions that are encountered by railroad tank cars. Executing a systematic characterization effort is important to avoid the situation shown in Figure 1. The wide scatter in FCG rate at a given ΔK , in this case for A36 steel using numerous datasets from the literature⁽⁶⁾, is a source of enormous uncertainty in a deterministic life prediction.

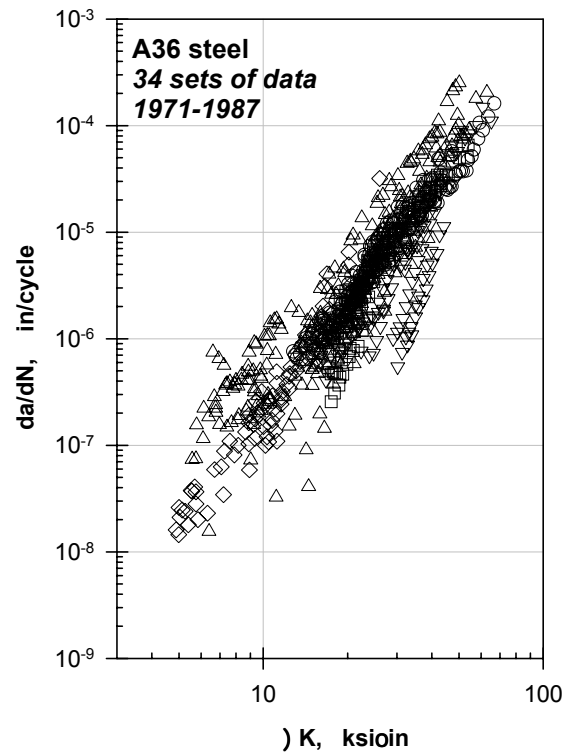


Figure 1. FCG data scatter for A36 steel.

MATERIALS AND METHODS

Materials: Two tank car manufacturers supplied the plate material utilized during this program. The goal was to process the two materials in a similar fashion and simulate tank car material currently in-service. Material type A (from Bethlehem Steel) is 0.781-inch thick and was received in a normalized form. Material type B (from U.S. Steel) is 0.813-inch thick with better controlled low-temperature fracture toughness and is used in cold-temperature cars. Material B was double normalized by first heating to 1655°F, holding for 30 minutes and cooling to ambient temperature in still air followed by a repeat cycle at 1600°F. Both materials were subsequently stress relieved by introducing into a 600°F furnace, heating at 400°F/hour to 1125°F, holding for 60 minutes and cooling to 600°F at a rate no greater than 500°F/hour. Cooling to ambient temperature subsequently occurred in still air. The materials were stress relieved, since tank cars are stress relieved during manufacture after welding.

The chemistries and tensile properties of each material lot are indicated in Tables I and II, respectively. Even though the lots were from different suppliers, the basic chemistry and properties were quite similar and within AAR specifications for TC-128B. The double normalized type B material exhibited a slight (1-2 ksi) decrease in strength when compared to the single normalized type A material. However, it is unknown whether this is a consequence of different lots or the normalization scheme.

Table I. Measured chemistries for the two different materials and AAR TC-128B specification⁽⁷⁾.

Matl	C	Mn	P	S	Si	Cu	Ni	Cr	Mo	V	Al	Nb	Ti	B	N	Sn
A	.23	1.32	.023	.008	.37	.03	.01	.02	.07	.05	.03	<.01	<.01	<.0005	.0092	<.01
B	.23	1.33	.021	.006	.22	.05	.02	.17	.07	.07	.03	<.01	.01	<.0005	.0066	.01
spec	<.29	.92-1.62	<.035	<.040	.13-.45	<.35	<.25	<.25	<.08	<.08	-	-	-	-	-	-

Table II. Average room temperature tensile test properties of the two lots of TC-128B material used during testing.

Material	Orient	σ_{TS} , ksi	σ_{YS} , ksi	Elong, %	RA, %
A	L	85.4	58.8	29	63
	T	86.9	59.7	30	68
B	L	84.2	57.3	29	64
	T	84.5	57.9	31	69
AAR Specification		81-102	50 (min)	22 (min)	-

Experimental Methods: Fatigue crack growth rate testing was performed on 10-kip servohydraulic machines at frequencies between 5 and 20 Hz in accordance with the matrix of conditions in Table III. All testing was performed in lab air conditions with a relative humidity in the range of 40-75 percent. Fatigue crack growth experiments were performed in accordance with the ASTM E647 test specification⁽⁸⁾. In addition to the material lot difference, variables assessed include load ratio ($R = 0.1, 0.6$ and -1.0), orientation (L-T and L-S) and, indirectly, crack growth test technique (K-decreasing, -increasing, constant- K_{max} with increasing- K_{min}). Recall, the K-decreasing and -increasing tests are (executed sequentially) performed at a fixed R-ratio whereas the constant- K_{max} , increasing- K_{min} tests (for threshold level estimation)

vary from $R = 0.1$ (at high ΔK) to $R = 0.9$ at the completion of testing when ΔK approaches threshold. During constant K_{\max} testing, K_{\max} was fixed at 30 ksi $\sqrt{\text{in}}$.

The specimen thickness ranged from 0.225 to 0.250 inch. Three specimen geometries were employed: a 3-inch wide compact tension, C(T), specimen, a 4-inch wide middle cracked tension, M(T), specimen and a 0.75-inch wide single edge notched bend, SE(B) specimen. The two geometries other than the standard C(T) were utilized to accommodate $R < 0$ cycling, M(T), and testing in the thickness direction SE(B). The compacts and middle cracked tension specimens were in the L-T orientation whereas the bend specimens were in the L-S orientation. All tests were performed in automated K-control using an FTA (Fracture Technology Associates, Bethlehem, PA) external computer control system. Although visual crack length measurements were periodically taken on all specimens, compliance (for the compact and bend specimens) and indirect PD [M(T) specimens] were used to control the test. Non-visual crack length measurements were extensively validated during testing. In addition, back-face strain gages were used on the four-point bend and compact tension specimens to assist understanding closure conditions (however, crack closure results are beyond the scope of this paper).

Table III. Summary of all of the fatigue crack growth tests performed during this testing.
The symbol “ \rightarrow ” denotes constant conditions.

Test ID	Type of Test Specimen			Matl Lot	Load Ratio, R	Type of Test Performed			
	C(T)	M(T)	SE(B)			$\Delta K \downarrow$	$\Delta K \uparrow$	$\rightarrow K_{\max}$	$\uparrow K_{\min}$
TC-A-1A	✓			A	0.1	✓	✓		
TC-B-1A	✓			B	0.1	✓	✓		
TC-A-1B	✓			A	0.1	✓	✓		
TC-B-1B	✓			B	0.1	✓	✓		
TC-A-2A	✓			A	0.6	✓	✓		
TC-B-2A	✓			B	0.6	✓	✓		
TC-A-2B	✓			A	0.1-0.9				✓
TC-A-6		✓		A	-1.0	✓			
TC-A-7		✓		A	-1.0	✓	✓		
TC-A-9			✓	A	0.1	✓			
TC-A-10			✓	A	0.1		✓		
TC-A-11			✓	A	0.1-0.9				✓
TC-A-12			✓	A	0.1		✓		

RESULTS AND DISCUSSION

Prior to examining the results, it is worthwhile to briefly review typical guidelines regarding repeatability in fatigue crack growth rate tests. A careful study of the ASTM standard⁽⁸⁾ suggests that typical FCG rate variability is approximately a factor of 2x for a given ΔK level. However, the round robin during which this factor was developed occurred over 25 years ago and it is believed that repeatability has improved since that time*.

K-Gradient and Material Lot Effects: The pre-test expectation was that the effects of both of these variables would be slight. Nevertheless, it is critically important to experimentally assess this supposition.

* As an aside, ASTM committee E08 is currently re-evaluating the issue of variability and performing a new round robin on FCG testing.

Some representative test data are shown for a two segment (K-decreasing and -increasing) high R-ratio specimen in the L-T orientation in Figure 2. When performing K-gradient testing, it is important to ensure that the load history defined by the value of C , where $C = dK/Kda$, does not influence the test results appreciably. It is clear from Figure 2 that the K-decreasing ($C < 0$) segment agrees remarkably well with the K-increasing segment. These data also indicate (a) how well the material replicates FCG behavior in the Paris region and (b) the excellent level of control achieved during the test. The obvious conclusion from Figure 2 is that the C values chosen for the decreasing and increasing segments are suitable and do not bias the FCG results.

Scatter in fatigue crack growth rates such as that shown for A36 data in Figure 1 is often attributed to material lot variability. Admittedly, A36 steel is not a tightly controlled grade and the data in Figure 1 samples a wide range of variables including load ratio, orientation, temperature, corrosive environments and welds (note that all of these variables are commonly encountered in tank car structure). Nevertheless, the small influence of material lot (Type A or B) on FCG properties for TC-128B is apparent from the low and high R-ratio data shown in Figure 3. The data for each material at each stress ratio consists of results from both increasing- and decreasing- ΔK tests. The similarity between the FCG responses for Type A and B material is striking. At the lower R-ratio, greater variability, both within and between the datasets, is apparent. At higher R-ratio, when one expects less effects of crack closure (a contributor to variability), the agreement between the material response is excellent.

Orientation and R-ratio Effects: Conventional wisdom about fatigue suggests that the influence of these variables should be greater than observed for the variables examined so far. Data from the in-plane L-T and through-thickness L-S orientation is shown for $R = 0.1$ in Figure 4. Although a greater level of variability is noted for the L-S orientation (now more in accordance with ASTM guidelines at the higher growth rates), a clear difference between the two orientations is evident, especially in the Paris regime at higher ΔK levels. The FCG rates are slower in the L-S orientation, *i.e.*, as the fatigue crack grows through the thickness of the material. This is significant since a high percentage of cracks in tank cars are typically surface initiated (due to bending or residual stress effects) and grow through the thickness of the tank.

Constant R-ratio test results are contrasted in Figure 5 with the constant K_{\max} test data where, recall, the R-ratio is increased from 0.1 to 0.9 as ΔK is decreased. In the Paris regime of the data, the difference between low and high fixed R-ratio data is slight, typically on the order of 2x or less. This difference increases as the FCG rate decreases to less than 10^{-7} inch/cycle, regardless of orientation. The constant- K_{\max} FCG data in the L-T orientation follows expectation by mirroring the low R data at the start of the test (at high ΔK) and then following the high R data until close to threshold. The high R-ratio threshold for the L-T orientation is in the range of 2-3 ksi $\sqrt{\text{in}}$ whereas at low R-ratio it appears more on the order of 5-6 ksi $\sqrt{\text{in}}$. This trend is consistent with typical material behavior where ΔK_{th} decreases as R-ratio increases. This

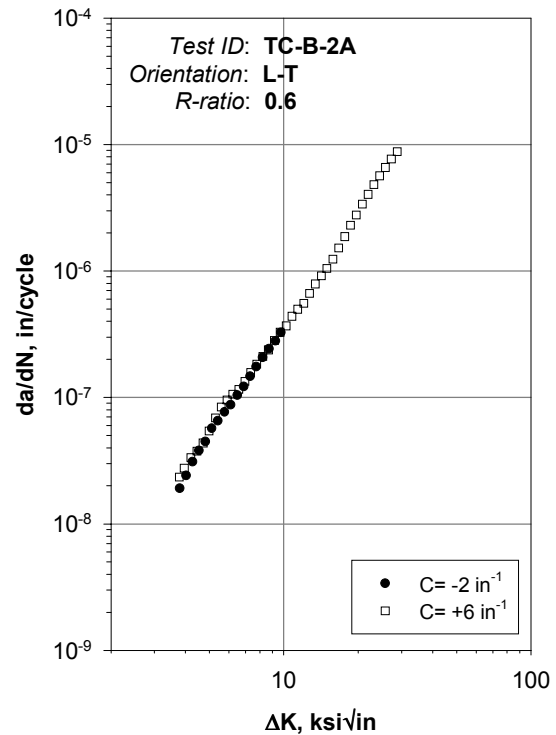


Figure 2. Effect of K-gradient on FCG behavior.

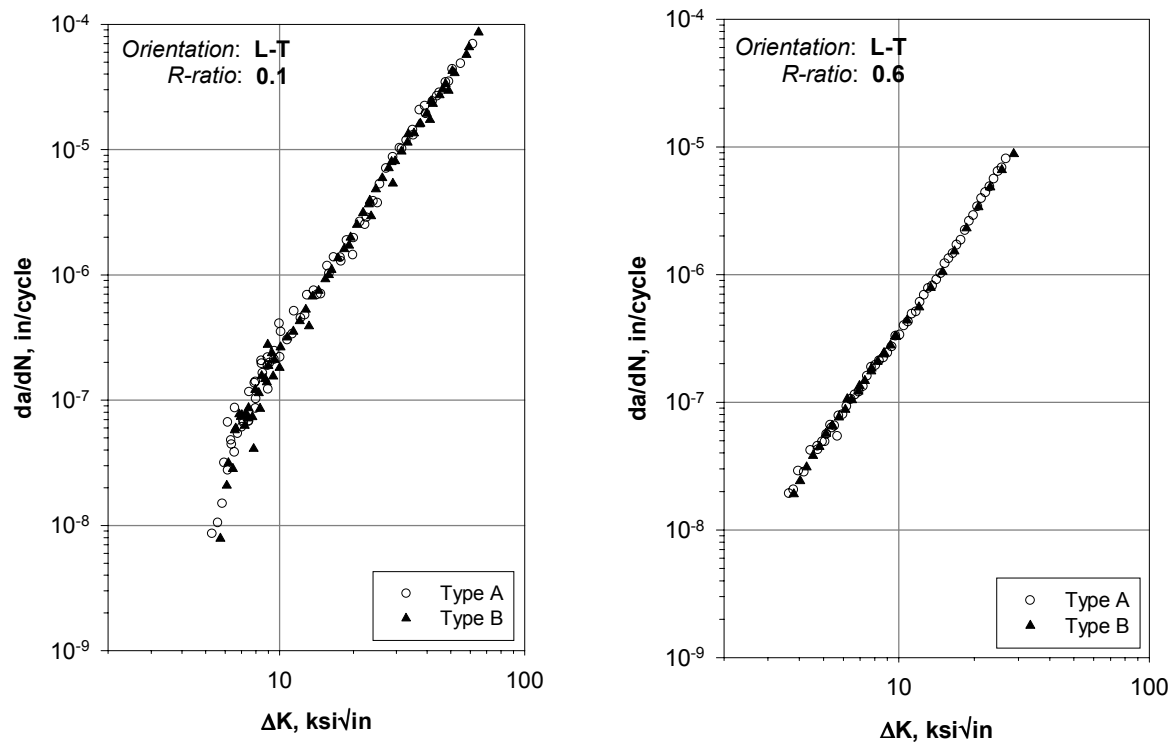


Figure 3. Effect of material lot on FCG behavior at both low and high R-ratio.

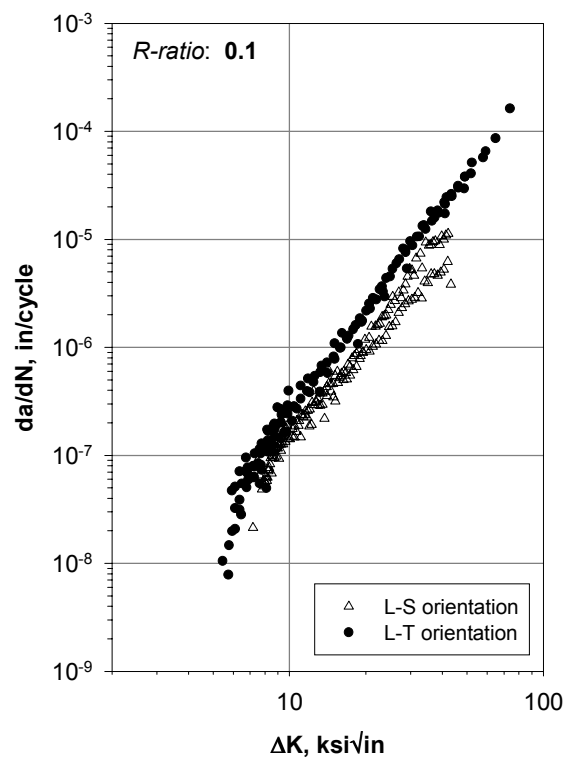


Figure 4. Influence of orientation on FCG behavior.

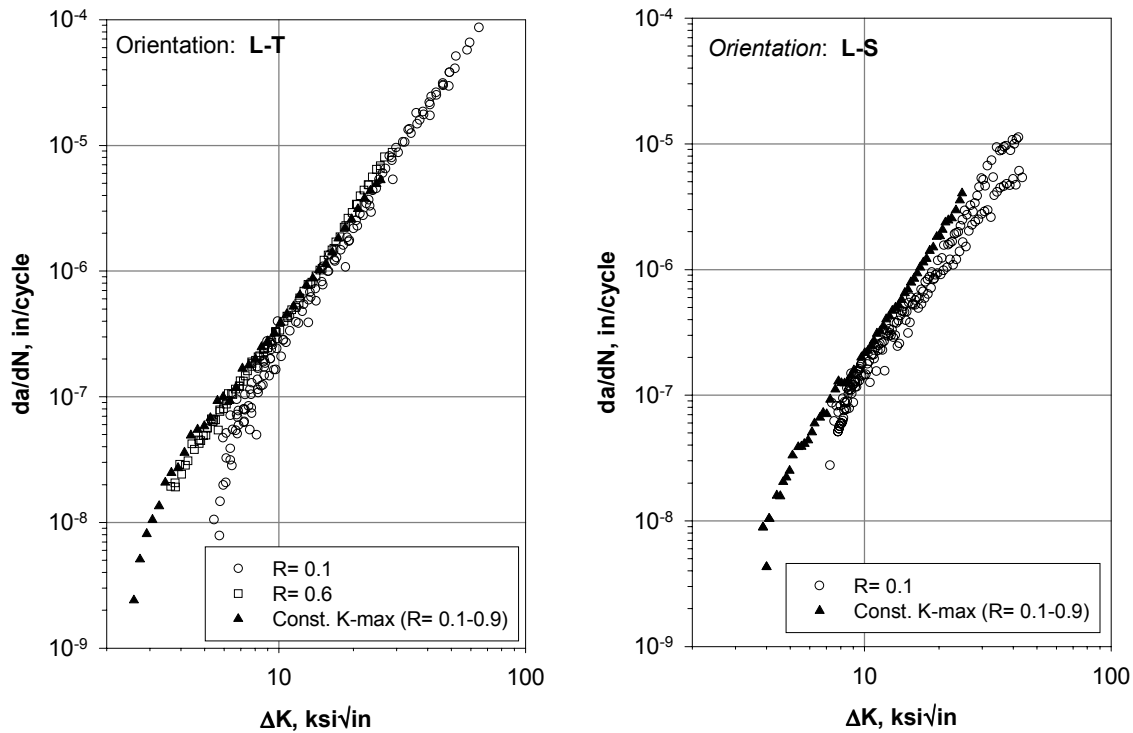


Figure 5. Comparison between fixed R-ratio and constant K_{\max} FCG data for the L-T and L-S orientation.

behavior for the L-T orientation is contrasted to the L-S case in Figure 5 where the constant- K_{\max} data suggests a high R-ratio threshold of 3-4 $\text{ksi}\sqrt{\text{in}}$.

Negative R-ratio data is shown with the previous L-T data from Figure 5 in Figure 6. Although the data appears somewhat obscured from the other datasets on the plots, a careful observation of Figure 6 will show that the $R = -1$ data typically exhibits the lowest growth rates for all conditions at a given ΔK . However, the overall difference between positive and negative R-ratio is slight. Nevertheless, the observed trend for tension-compression loading conditions is consistent with that observed in other materials, including light alloys and steels, although the effect in most materials tends to be greater than the data shown herein.

Comparison of FCG Data with Other Sources: The fatigue crack growth data shown so far exhibits excellent repeatability and all general trends are in accordance with expectation. It is rare that the fatigue crack growth behavior of a candidate material is as well characterized as the TC-128B studied herein. In this case, someone performing a DTA must use one of the empirical relationships derived for steel. Three

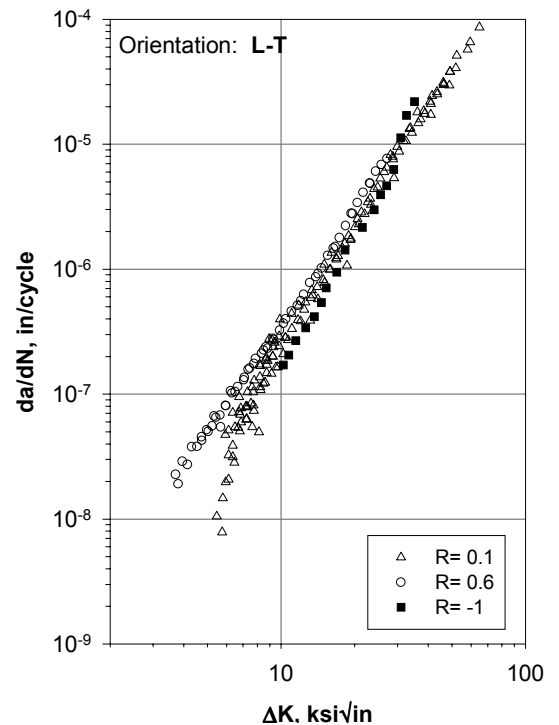


Figure 6. FCG data for all R-ratio (L-T).

relationships that are available⁽⁹⁻¹¹⁾, were used for different strength levels and classifications of steel. Nevertheless, an examination of each clearly indicates that all are fairly similar. The most conservative of these relations (in terms of predicting a slightly higher fatigue crack growth rate at a given ΔK level) is that derived by Hudak, Burnside and Chan⁽⁹⁾ (HBC) for structural and low alloy steels. This empirical relationship, divided up into low and high R-ratio behavior ($R > 0.5$) is shown with the constant- K_{max} FCG data for the L-T and L-S orientations in Figure 7.

The L-T data in Figure 7 follows with expectation: at the start of the constant- K_{max} test (*i.e.*, at high ΔK) the data is on the low R-ratio HBC line and the test progresses and the data clearly moves toward the high R-ratio line, only diverging as ΔK decreases toward threshold. The data for the L-S orientation is clearly different. Even though R varied from 0.1 to 0.9 during the test, the data remains underneath the low R HBC line. This suggests that (a) the L-S orientation exhibits very slight R-ratio effects (since the data is parallel to the HBC relation) and (b) the observed growth rate in the L-S orientation is slower than predicted by the HBC relationship.

Prior to the earlier described damage tolerance effort, the tank car industry did not require FCG data for TC-128B material. Therefore, to our knowledge, no FCG data other than that shown herein is believed to exist for TC-128B. However, A612 material is fairly similar in composition and overall mechanical properties, although the microstructure and toughness are not as well controlled in A612 as in TC-128B. A survey of the literature identified A612 FCG data in a reference from Poon and Hoepfner⁽¹²⁾. These data are plotted in Figure 8 with the TC-128B data band from the $R = 0.1$ and 0.6 data in Figure 6. Although the scatter in the literature data appears greater than in the current data, the overall trend agrees reasonably well. Although it is difficult to tell definitively, the difference between FCG rates at R of 0.1 and 0.6 in the Poon data may actually be less than we observed herein.

The observation of comparable fatigue crack growth properties when contrasting 2000 vintage TC-128B and 1977 vintage A612 is an interesting observation from the viewpoint of the aging tank car fleet. A recent

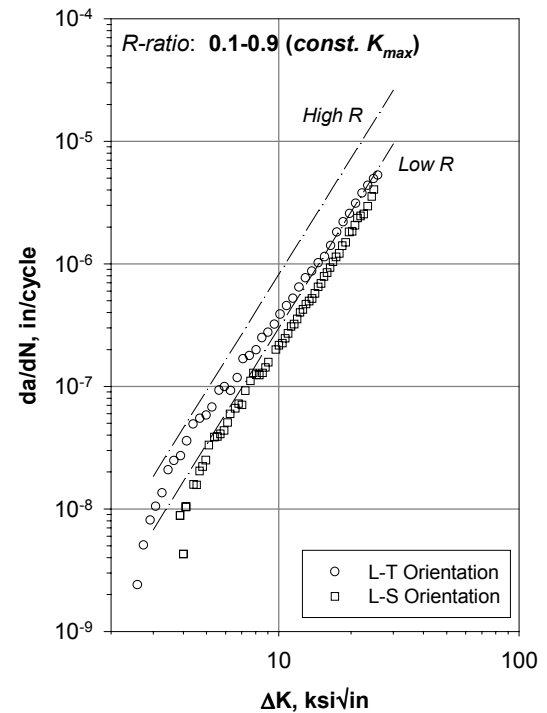


Figure 7. Comparison to HBC relation⁽⁹⁾.

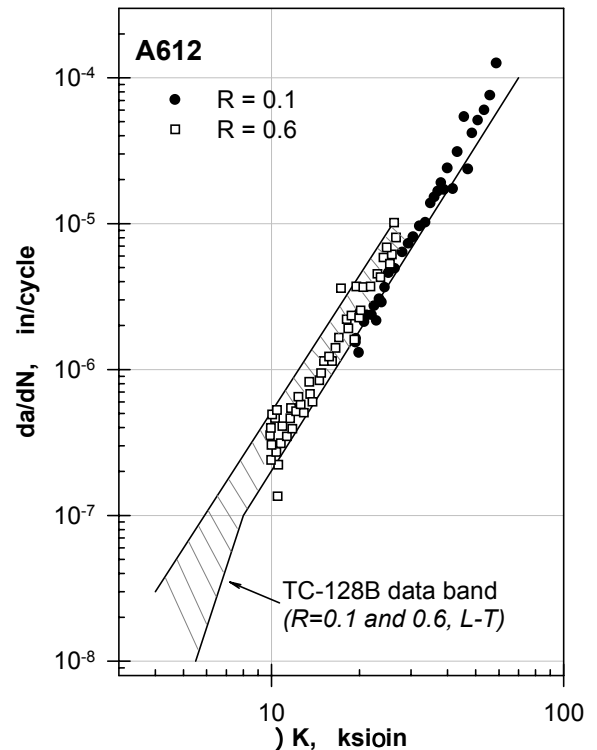


Figure 8. Comparison to literature data⁽¹²⁾.

source⁽¹³⁾ indicates the average age of privately operated tank carts is 16.6 years with 42 percent of the fleet built more than 20 years ago. If the A612 surveyed by Poon is consistent with the same vintage TC-128B, the FCG properties measured herein might be applicable to older TC-128B tanks in the fleet, not just the newer generation. The hypothesized link between fatigue properties of 25-year-old A612 and those of similar vintage TC-128B is as yet unsubstantiated. However, this is a reasonable possibility and worthy of further attention.

The data included herein provides a baseline assessment of the FCG behavior of TC-128B. Using relations derived from these data in a DTA analysis is clearly more optimum than a standard relationship such as the HBC model since it will yield more accurate life prediction. Nevertheless, it is worth noting that the data agrees generally with the HBC model and A612 data from the literature. One clear feature of this work is that the data extends all the way down to near threshold, a regime not included in any of the models in References 9-11 and critically important for accurate life prediction. Another significant aspect of these data is FCG behavior in the L-S orientation which is the critical orientation of primary concern if the objective is to prevent lading leakage. Furthermore, the influence of environmental variables such as moisture level and temperature on FCG properties is the subject of an ongoing effort extending these results. Finally, issues such as welds and variable amplitude loading influence FCG behavior in an as yet undetermined manner.

CONCLUSIONS

The fatigue crack growth behavior of TC-128B steel has been examined in detail herein. Two different lots of TC-128B material, each in accordance with chemical and mechanical property guidelines, were tested and found to yield consistent FCG properties. The different K-gradient methods applied, although in the strict sense outside the ASTM E647 guidelines, were shown to yield repeatable FCG data that was independent of the K-gradients used where other conditions were held constant. Moreover, the effects of R-ratio and specimen orientation both yield an overall 2x factor on FCG rate for ΔK in the Paris regime: higher R-ratio data exhibited faster rates than low R-ratio data and the in-plane L-T orientation exhibited a faster growth rate than the through-thickness L-S orientation. The high R-ratio threshold behavior for the two orientations were of similar magnitude: 2-3 ksi $\sqrt{\text{in}}$ and 3-4 ksi $\sqrt{\text{in}}$ for the L-T and L-S orientation, respectively. As the FCG threshold was approached, the effects of R-ratio and orientation generally increased. Finally, a favorable comparison was made between the TC-128B FCG data measured herein and several data representations from the literature.

ACKNOWLEDGEMENTS

This research was supported by the Federal Railroad Administration Office of Research and Development, program manager Ms. Claire Orth. Mr. Jose Pena is the project manager for FRA research related to tank car safety. Appreciation is extended to Union Tank Car Company (Phil Daum, Al Henzi and Frank Reiner) and Trinity Industries (Tom Dalrymple) for donating the material used during this testing. The tireless efforts of Messrs. Dale Haines, Darryl Wagar, Harold Saldaña, Rick Fess and Forrest Campbell are kindly appreciated. Gratitude is also extended to Ms. Loretta Mesa for the assistance in preparing this manuscript.

REFERENCES

1. "Inspection and Testing of Railroad Tank Cars," NTSB/SIR-92/05, National Transportation Safety Board, Washington, D.C., 1992.
2. J. P. Gallagher, *et al.*, "USAF Damage Tolerant Design Handbook," AFWAL-TR-82-3073, May 1984.
3. "Damage Tolerance Assessment Handbook," Vols. I and II, DOT-VNTSC-FAA-93-13.I, Oct. 1993.
4. P. C. Paris, M. P. Gomez, and W. P. Anderson, "A Rational Analytic Theory of Fatigue," The Trend in Engineering, University of Washington, 1961.
5. S. Suresh, Fatigue of Materials, Cambridge University Press, Cambridge, UK, 1991.
6. J. W. Cardinal, P. C. McKeighan, and S. J. Hudak, "Damage Tolerance Analysis of Tank Car Stub Sill Cracking," Southwest Research Institute Final Report No. 06-6965, prepared for the Tank Car Stub Sill Working Group, Nov. 1998.
7. "Appendix M – Specifications for Materials," Manual of Standards and Recommended Practices, Section C – Part III, Specifications for Tank Cars, Specification M1002, The Association of American Railroads, Sept. 1992.
8. Annual Book of ASTM Standards, Section 3: Metals Test Methods and Analytical Procedures, Vol. 3.01, American Society for Testing and Materials, West Conshohocken, PA, 2000.
9. S. J. Hudak, Jr., O. H. Burnside, and K. S. Chan, "Analysis of Corrosion Fatigue Crack Growth in Welded Tubular Joints," Journal of Energy Resources Technology, ASME, Vol. 107, June 1985.
10. E. D. Eason, J. D. Gilman, D. P. Jones, and S. P. Andrew, "Technical Basis for a Revised Crack Growth Rate Reference Curve for Ferritic Steels in Air," Journal of Pressure Vessel Technology, ASME, Vol. 114, Feb. 1992.
11. N. Yazdani and P. Albrecht, "Crack Growth Rates of Structural Steel in Air and Aqueous Environments," Engineering Fracture Mechanics, Vol. 32, No. 6, 1989, pp. 997-1007.
12. C. Poon and C. W. Hoeppner, "The Effect of Temperature and R Ratio on Fatigue Crack Growth in A612 Grade B Steel," Engineering Fracture Mechanics, Vol. 12, 1979, pp. 23-31.
13. Progressive Railroading, Vol. 44, No. 5, Trade Press Publishing Corporation, May 2001.